

# Accurate calibration of relativistic mean-field models: correlating observables and providing meaningful theoretical uncertainties

F. J. Fattoyev<sup>1,2,\*</sup> and J. Piekarewicz<sup>1,†</sup>

<sup>1</sup>*Department of Physics, Florida State University, Tallahassee, FL 32306*

<sup>2</sup>*Institute of Nuclear Physics, Tashkent 100214, Uzbekistan*

(Dated: February 18, 2022)

Theoretical uncertainties in the predictions of relativistic mean-field models are estimated using a chi-square minimization procedure that is implemented by studying the small oscillations around the chi-square minimum. By diagonalizing the matrix of second derivatives, one gains access to a wealth of information—in the form of powerful correlations—that would normally remain hidden. We illustrate the power of the *covariance analysis* by using two relativistic mean-field models: (a) the original linear Walecka model and (b) the accurately calibrated FSUGold parametrization. In addition to providing meaningful theoretical uncertainties for both model parameters and predicted observables, the covariance analysis establishes robust correlations between physical observables. In particular, we show that whereas the correlation coefficient between the slope of the symmetry energy and the neutron-skin thickness of Lead is indeed very large, a 1% measurement of the neutron radius of Lead may only be able to constrain the slope of the symmetry energy to about 30%.

PACS numbers: 21.60.Jz, 21.65.Cd, 21.65.Mn

## I. INTRODUCTION

The need to provide meaningful uncertainties in theoretical predictions of physical observables is a theme that is gaining significant momentum among the scientific community. Indeed, the search for a microscopic theory that both predicts and provides well-quantified theoretical uncertainties is one the founding pillars of the successful UNEDF collaboration [1]. Moreover, as recently articulated in an editorial published in the Physical Review A [2], theoretical predictions submitted for publication are now expected to be accompanied by meaningful uncertainty estimates. The need for “*theoretical error bars*” becomes particularly critical whenever models calibrated in certain domain are used to extrapolate into uncharted regions.

Although firmly rooted in QCD, computing both the nucleon-nucleon (NN) interaction and the properties of nuclei in terms of the underlying quark and gluon constituents remains a daunting task. Hence, rather than relying strictly on QCD, one uses the properties of QCD (such as chiral symmetry and relevant energy scales) as a guide to construct phenomenological interactions using nucleons and mesons as the fundamental degrees of freedom. However, QCD has little to say about the strength of the underlying model parameters which must then be constrained from experimental data. For example, deuteron properties along with two-body scattering data are used to build a nucleon-nucleon interaction that may then be used (supplemented with a phenomenological three-body force) to compute *ab-initio* the properties of light nuclei. Attempting *ab-initio* calculations of the properties of medium-to-heavy nuclei remains well beyond the scope of the most powerful computers to date. In this case one must bring to bear the full power of density functional theory (DFT). Following the seminal work by Kohn and collaborators [3], DFT shifts the focus from the complicated many-body wave-function to the much simple one-body density. Moreover, Kohn and Sham have shown how the one-body density may be obtained from a variational problem that reduces to the solution of a set of mean-field-like (“*Kohn-Sham*”) equations [4]. The form of the Kohn-Sham potential is in general reminiscent of the underlying (bare) NN potential. However, the constants that parametrize the Kohn-Sham potential are directly fitted to many-body observables (such as masses and charge radii) rather than two-body data. In this manner the complicated dynamics originating from exchange and correlation effects get implicitly encoded in the empirical constants. Yet regardless of whether the effective interaction is fitted to two-nucleon or to many-body data—the determination of the model parameters often relies on the optimization of a quality measure.

In this contribution we focus on density functional theory and follow the standard protocol of determining the model parameters through a  $\chi^2$ -minimization procedure. This procedure is implemented by: (a) selecting a set of accurately measured ground-state observables and (b) demanding that the differences between these observables and

---

\*Electronic address: ff07@fsu.edu

†Electronic address: jpiekarewicz@fsu.edu

the predictions of the model be minimized. Note that in the present framework a model consists of both a set of parameters and a  $\chi^2$ -measure. In general, modifying the  $\chi^2$ -measure (e.g., by adding observables) results in a change in the model parameters. Traditionally, once the  $\chi^2$ -minimum has been found one proceeds to validate the model against observables not included in the quality fit. Nuclear collective excitations are a potentially “safe” testing arena for the model as they represent the *small oscillations* around the variational ground state. But what happens when the model must be extrapolated to regions of large isospin imbalance and high density as in the interior of neutron stars? Clearly, without reliable theoretical uncertainties it is difficult to assess the predictions of the model. To remedy this situation we propose to study the *small oscillations* around the  $\chi^2$ -minimum—rather than the minimum itself. As we shall see, such a statistical analysis—inspired by the recent study reported in Ref. [5]—provides access to a wealth of information that remains hidden if one gets trapped in the  $\chi^2$ -minimum. Among the critical questions that we will be able to answer is how fast does the  $\chi^2$ -measure deteriorate as one moves away from the minimum. Should additional observables be added to the  $\chi^2$ -measure to better constrain the model? And if such observables are hard to determine are there others that may be more readily accessible and provide similar constraints? A particularly topical example that illustrates such a synergy is the correlation between the neutron-skin thickness and electric dipole polarizability of neutron-rich nuclei [5, 6]. A detailed analysis of such correlation—which involves a systematic study of the isovector dipole response—is beyond the scope of this initial study and will become the subject of a forthcoming publication. Yet the study of correlations among observables sensitive to the poorly-determined density dependence of the symmetry energy will become a recurring theme throughout this contribution.

The manuscript has been organized as follows. In Sec. II we develop the necessary formalism to implement the correlation analysis. This section is divided in two parts: (a) a discussion on the structure of a class of relativistic mean-field models and (b) a relatively short—yet fairly complete—derivation of the statistical formalism required to perform the covariance analysis. In Sec. III two simple examples are used to illustrate the power of the formalism. This exercise culminates with the estimation of meaningful theoretical error bars and correlation coefficients. Our conclusions and outlook are presented in Sec. IV.

## II. FORMALISM

In this section we develop the formalism required to implement the correlation analysis. First, in Sec. II A we introduce a fairly general class of relativistic mean-field models that are rooted in effective-field-theory concepts, such as naturalness and power counting. Second, in Sec. II B we present a self-contained derivation of the ideas and formulas required to implement the covariance analysis.

### A. Relativistic Mean-Field Models

Relativistic mean-field models traditionally include an isodoublet nucleon field ( $\psi$ ) interacting via the exchange of two isoscalar mesons (a scalar  $\phi$  and a vector  $V^\mu$ ), one vector-isovector meson ( $b^\mu$ ), and the photon ( $A^\mu$ ) [7–9]. The non-interacting Lagrangian density for such a model may be written as follows:

$$\begin{aligned} \mathcal{L}_0 = & \bar{\psi} (i\gamma^\mu \partial_\mu - M) \psi + \frac{1}{2} \partial_\mu \phi \partial^\mu \phi - \frac{1}{2} m_s^2 \phi^2 \\ & - \frac{1}{4} V^{\mu\nu} V_{\mu\nu} + \frac{1}{2} m_v^2 V^\mu V_\mu - \frac{1}{4} \mathbf{b}^{\mu\nu} \cdot \mathbf{b}_{\mu\nu} + \frac{1}{2} m_\rho^2 \mathbf{b}^\mu \cdot \mathbf{b}_\mu - \frac{1}{4} F^{\mu\nu} F_{\mu\nu} , \end{aligned} \quad (1)$$

where  $V_{\mu\nu}$ ,  $\mathbf{b}_{\mu\nu}$ , and  $F_{\mu\nu}$  are the isoscalar, isovector, and electromagnetic field tensors, respectively. That is,

$$V_{\mu\nu} = \partial_\mu V_\nu - \partial_\nu V_\mu , \quad (2a)$$

$$\mathbf{b}_{\mu\nu} = \partial_\mu \mathbf{b}_\nu - \partial_\nu \mathbf{b}_\mu , \quad (2b)$$

$$F_{\mu\nu} = \partial_\mu A_\nu - \partial_\nu A_\mu . \quad (2c)$$

The four constants  $M$ ,  $m_s$ ,  $m_v$ , and  $m_\rho$  represent the nucleon and meson masses and may be treated (if wished) as empirical parameters. Often, however,  $m_s$  is determined from an accurate calibration procedure. The interacting Lagrangian density has evolved significantly over the years and now incorporates a variety of meson self-interacting terms that are designed to improve the quality of the model. Following ideas developed in Ref. [9] we write the interacting Lagrangian density in the following form:

$$\mathcal{L}_{\text{int}} = \bar{\psi} \left[ g_s \phi - \left( g_v V_\mu + \frac{g_\rho}{2} \boldsymbol{\tau} \cdot \mathbf{b}_\mu + \frac{e}{2} (1 + \tau_3) A_\mu \right) \gamma^\mu \right] \psi - U(\phi, V_\mu, \mathbf{b}_\mu) . \quad (3)$$

In addition to the standard Yukawa interactions, the Lagrangian is supplemented with an effective potential  $U(\phi, V_\mu, \mathbf{b}_\mu)$  consisting of non-linear meson interactions that serve to simulate the complicated dynamics that lies beyond the realm of the mean-field theory. Indeed, by fitting the various coupling constants directly to nuclear properties—rather than to two-nucleon data—the complicated dynamics originating from nucleon exchange, short-range effects, and many-body correlations gets implicitly encoded in a small number of parameters. For the purpose of the present discussion we introduce explicitly all non-linear terms up to fourth-order in the meson fields. That is,

$$U(\phi, V^\mu, \mathbf{b}^\mu) = \frac{\kappa}{3!}\Phi^3 + \frac{\lambda}{4!}\Phi^4 - \frac{\zeta}{4!}(W_\mu W^\mu)^2 - \Lambda_v(W_\nu W^\nu)(\mathbf{B}_\mu \cdot \mathbf{B}^\mu) - \frac{\xi}{4!}(\mathbf{B}_\mu \cdot \mathbf{B}^\mu)^2 \quad (4)$$

$$+ \kappa_0 \Phi W_\mu W^\mu + \kappa_1 \Phi \mathbf{B}_\mu \cdot \mathbf{B}^\mu + \lambda_0 \Phi^2 W_\mu W^\mu + \lambda_1 \Phi^2 \mathbf{B}_\mu \cdot \mathbf{B}^\mu - \Lambda'_v(W_\mu W_\nu)(\mathbf{B}^\mu \cdot \mathbf{B}^\nu) + \dots$$

where the following definitions have been introduced:  $\Phi \equiv g_s \phi$ ,  $W_\mu \equiv g_v V_\mu$ , and  $\mathbf{B}_\mu \equiv g_\rho \mathbf{b}_\mu$ . Given that the present analysis will be restricted to the study of uniform nuclear matter, terms proportional to the derivatives of the meson fields have not been included. As it stands, the relativistic model contains 14 undetermined parameters (1 meson mass, 3 Yukawa couplings, and 10 meson self-interaction terms). Note that if one incorporates the occasionally-used scalar-isovector  $\delta$ -meson [10, 11], then 9 additional parameters must be included to this order (1 Yukawa coupling, and 8 meson self-interaction terms).

A model with 14—or 23—parameters goes significantly beyond the early relativistic models that were able to reproduce the saturation point of symmetric nuclear matter as well as various ground-state observables with only a handful of parameters (a single meson mass and three Yukawa couplings) [7, 12, 13]. Although fairly successful, those early models suffered from a major drawback: an unrealistically large incompressibility coefficient. Such a problem was successfully solved by Boguta and Bodmer with the introduction of cubic and quartic scalar meson self-interactions [14]. Remarkably, using only these six parameters ( $m_s, g_s, g_v, g_\rho, \kappa, \lambda$ ) it is possible to reproduce a host of ground-state properties of finite nuclei (both spherical and deformed) throughout the periodic table [15, 16]. And by adding two additional parameters ( $\zeta$  and  $\Lambda_v$ ) the success of the model can be extended to the realm of nuclear collective excitations and neutron-star properties [17–20].

Given that the existent database of both laboratory and observational data appears to be accurately described by an 8-parameter model, is there any compelling reason to include 6—or 15—additional parameters? And if so, what criteria does one use to constrain these remaining parameters? A meaningful criterion used to construct an effective Lagrangian for nuclear-physics calculations has been proposed by Furnstahl, Serot, and Tang based on the concept of “*naive dimensional analysis*” and “*naturalness*” [21, 22]. The basic idea behind naturalness is that once the *dimensionful* meson fields (having units of mass) have been properly scaled using strong-interaction mass scales, the remaining *dimensionless* coefficients of the effective Lagrangian should all be “*natural*”; that is, neither too small nor too large [21, 23]. Such an approach is both useful and powerful as it allows an organizational scheme based on an expansion in powers of the meson fields. Terms in the effective Lagrangian with a large number of meson fields will then be suppressed by a large strong-interaction mass scale. In this regard the assumption of naturalness is essential as the suppression from the large mass scale should not be compensated by large, *i.e.*, unnatural, coefficients. It was by invoking the concept of naturalness that we were able to truncate the effective potential  $U(\phi, V^\mu, \mathbf{b}^\mu)$  beyond quartic terms in the meson fields.

Although we have justified the truncation of the effective Lagrangian invoking naturalness, we are not aware of an additional organizational principle that may be used *a-priori* to limit further the form of  $U(\phi, V^\mu, \mathbf{b}^\mu)$ . This implies that *all* model parameters must be retained, as it is unnatural to set some coefficients arbitrarily to zero without a compelling symmetry argument [24]. In principle then, all model parameters must be retained and subsequently determined from a fit to empirical data. In practice, however, many successful theoretical models—such as NL3 [15, 16] and FSUGold [18]—arbitrarily set some of these parameters to zero. The “*justification*” behind these fairly ad-hoc procedure is that whereas the neglected terms are of the same order in a power-counting scheme, the full set of parameters is poorly determined by existing data, so ignoring a subset model parameters does not compromise the quality of the fit [9, 21].

An important goal of the present work is to investigate correlations among the parameters of the model and whether additional physical observables could remove such correlations. To do so we follow the standard protocol of determining the model parameters through a  $\chi^2$  minimization procedure. Traditionally, this procedure is implemented by selecting a set of accurately measured ground-state observables for a variety of nuclei and then demanding that the differences between the observables and the predictions of the model be minimized. Once this is done, the success of the model may be gauged by computing observables not included in the fit. However, it is often difficult to assess the uncertainty in the predictions of the model. To address this deficiency we propose to study the *small oscillations* around the minimum—rather than the minimum itself. Such a study—inspired by the recent statistical analysis presented in Ref. [5]—provides access to a wealth of information that, in turn, enables one to specify meaningful theoretical error bars as well as to explore correlations among model parameters and calculated observables.

Although the following discussion is framed in the context of an underlying  $\chi^2$ -measure, our arguments are general as they merely rely on the existence of a (local) minimum (or an extremum). As in any small-oscillations problem, deviations of the  $\chi^2$ -measure from its minimum value are controlled by a symmetric  $F \times F$  matrix, where  $F$  represents the total number of model parameters. Being symmetric, such a matrix may be brought into a diagonal form by means of an orthogonal transformation. The outcome of such a diagonalization procedure is a set of  $F$  eigenvalues and  $F$  eigenvectors. When a point in parameter space is expanded in terms of these eigenvectors, the deviations of the  $\chi^2$ -measure from its minimum value take the form of a system of  $F$  *uncoupled harmonic oscillators*—with the eigenvalues playing the role of the  $F$  spring constants. The spring constants may be “stiff” or “soft” depending on whether the curvature around the minimum is steep or shallow, respectively. As one explores the parameter landscape along a stiff direction—and thus along a particular linear combination of model parameters—a rapid worsening of the  $\chi^2$ -measure ensues, suggesting that the fitting protocol is robust enough to constrain this particular linear combination. Conversely, no significant deterioration in the quality of the fit is observed as one moves along a soft direction. In this case the  $\chi^2$ -minimum is of little significance as scores of parameter sets (*i.e.*, models) of nearly equal quality may be generated. This situation derives from the lack of certain critical observables in the  $\chi^2$ -measure. As we shall see, the particular linear combination of model parameters defining the soft direction often provides enough hints to identify the missing observable(s). Moreover, through this sort of analysis one may establish correlations among observables that are particularly sensitive to such soft directions. This is important as certain observables may be easier to measure than others. A particular topical case is that of the neutron-skin thickness in  $^{208}\text{Pb}$  and the electric dipole polarizability [5, 6, 25].

## B. Linear Regression and Covariance Analysis

As discussed earlier, relativistic models of nuclear structure are characterized by a number of model parameters, such as masses, Yukawa couplings, and non-linear meson coupling constants. Following the notation of Ref. [5], we denote a point in such a parameter space by  $\mathbf{p} = (p_1, \dots, p_F)$ , where  $F$  is the total number of model parameters. In principle, each value of  $\mathbf{p}$  represents a model. In practice, of course, one is ordinarily interested in the “best model” as defined by a quality measure. To do so, the model parameters are often calibrated to a well-determined set of ground-state properties of finite nuclei (such as masses and charge radii) that is supplemented by a few bulk properties of infinite nuclear matter (such as the binding energy, incompressibility coefficient, and symmetry energy at saturation density). Once the model parameters and the group of observables have been selected, the optimal parameter set is determined via a least-squares fit to the following  $\chi^2$  quality measure:

$$\chi^2(\mathbf{p}) = \sum_{n=1}^N \left( \frac{\mathcal{O}_n^{(\text{th})}(\mathbf{p}) - \mathcal{O}_n^{(\text{exp})}}{\Delta \mathcal{O}_n} \right)^2. \quad (5)$$

Here  $N$  (often much larger than  $F$ ) denotes the total number of selected observables whereas “th” and “exp” stand for the theoretical prediction and experimental measurement, respectively. Further, every observable is weighted by a factor of  $(\Delta \mathcal{O}_n)^{-1}$  that is (customarily) associated with the accuracy of the measurement.

We assume that—through a numerical procedure that is not of particular relevance to this work—an accurately-calibrated model  $\mathbf{p}_0$  has been found. This implies that all first derivatives of  $\chi^2$  vanish at  $\mathbf{p}_0$ . That is,

$$\left. \frac{\partial \chi^2(\mathbf{p})}{\partial p_i} \right|_{\mathbf{p}=\mathbf{p}_0} \equiv \partial_i \chi^2(\mathbf{p}_0) = 0 \quad (\text{for } i = 1, \dots, F). \quad (6)$$

The existence of the minimum (as opposed to a maximum or saddle point) also implies that a particular set of  $F$  second derivatives (to be defined shortly) must all be positive. Approaches based on a least-squares fit to a  $\chi^2$ -measure often culminate with the identification of the optimal parametrization  $\mathbf{p}_0$ . The predictive power of the model may then be appraised by computing observables that were not included in the fitting protocol. Less often, however, least-squares-fit approaches are used to evaluate the “uniqueness” of the model. In other words, how fast does the  $\chi^2$ -measure deteriorate as one moves away from  $\mathbf{p}_0$ ? Clearly, if the minimum is relatively flat (at least along one direction), then there will be little (or no) deterioration in the quality of the fit. Through a statistical analysis, we will be able to obtain a physically reasonable domain of parameters. We implement such analysis by studying the small oscillations around the  $\chi^2$ -minimum. As a bonus, we will be able to uncover correlations among observables and attach meaningful theoretical error bars to the theoretical predictions [5]. To start, we expand the  $\chi^2$ -measure around the optimal  $\mathbf{p}_0$  model. That is,

$$\chi^2(\mathbf{p}) = \chi^2(\mathbf{p}_0) + \frac{1}{2} \sum_{i,j=1}^F (\mathbf{p} - \mathbf{p}_0)_i (\mathbf{p} - \mathbf{p}_0)_j \partial_i \partial_j \chi^2(\mathbf{p}_0) + \dots \quad (7)$$

For convenience, we quantify the departure from the minimum by defining scaled, dimensionless variables

$$x_i \equiv \frac{(\mathbf{p} - \mathbf{p}_0)_i}{(\mathbf{p}_0)_i} . \quad (8)$$

In terms of these scaled variable, the quadratic deviations of the  $\chi^2$ -measure from its minimum value take the following compact form:

$$\chi^2(\mathbf{p}) - \chi^2(\mathbf{p}_0) \equiv \Delta\chi^2(\mathbf{x}) = \mathbf{x}^T \hat{\mathcal{M}} \mathbf{x} , \quad (9)$$

where  $\mathbf{x}$  is a column vector of dimension  $F$ ,  $\mathbf{x}^T$  is the corresponding transpose (row) vector, and  $\hat{\mathcal{M}}$  is the *symmetric*  $F \times F$  matrix of second derivatives defined by

$$\mathcal{M}_{ij} = \frac{1}{2} \left( \frac{\partial^2 \chi^2}{\partial x_i \partial x_j} \right)_{\mathbf{x}=0} = \frac{1}{2} (\mathbf{p}_0)_i (\mathbf{p}_0)_j \partial_i \partial_j \chi^2(\mathbf{p}_0) . \quad (10)$$

Being symmetric, the matrix  $\hat{\mathcal{M}}$  can be brought to a diagonal form by means of an orthogonal (change-of-basis) transformation. Denoting by  $\hat{\mathcal{A}}$  the orthogonal matrix whose columns are composed of the normalized eigenvectors and by  $\hat{\mathcal{D}} = \text{diag}(\lambda_1, \dots, \lambda_F)$  the *diagonal* matrix of eigenvalues, the following relation holds true:  $\hat{\mathcal{M}} = \hat{\mathcal{A}} \hat{\mathcal{D}} \hat{\mathcal{A}}^T$ . By inserting this relation into Eq. (9), we obtain the following simple and illuminating expression:

$$\Delta\chi^2(\mathbf{x}) = \mathbf{x}^T \left( \hat{\mathcal{A}} \hat{\mathcal{D}} \hat{\mathcal{A}}^T \right) \mathbf{x} = \boldsymbol{\xi}^T \hat{\mathcal{D}} \boldsymbol{\xi} = \sum_{i=1}^F \lambda_i \xi_i^2 . \quad (11)$$

Here the vector  $\boldsymbol{\xi} = \hat{\mathcal{A}}^T \mathbf{x}$  represents a point in parameter space expressed, not in terms of the original model parameters ( $g_s, g_v, \dots$ ) but rather, in terms of the new (“rotated”) basis. As previously advertised, the deviations of the  $\chi^2$ -measure from its minimum value have been parametrized in terms of  $F$  uncoupled harmonic oscillators—with the eigenvalues playing the role of the spring constants. In this way, each eigenvalue controls the deterioration in the quality of the fit as one moves along a direction defined by its corresponding eigenvector. A “soft” direction—characterized by a small eigenvalue and thus little deterioration in the  $\chi^2$  measure—involves a particular linear combination of model parameters that is poorly constrained by the choice of observables included in the least-squares fit. By isolating such linear combination(s) one can identify what kind of observables (e.g., isovector observables) should be added to the  $\chi^2$ -measure to better constrain the theoretical model. Moreover, one may also explore correlations among various observables (e.g., neutron-skin thickness and dipole polarizability) thereby facilitating the experimental extraction of some of these critical observables. This could be done by either refining existing experimental measurements or by designing brand new ones.

A concept of fundamental importance to the correlation analysis is the *covariance* between two observables  $A$  and  $B$ , denoted by  $\text{cov}(A, B)$  [26]. Assuming that  $(\mathbf{x}^{(1)}, \dots, \mathbf{x}^{(M)})$  represent  $M$  points (or models) in the neighborhood of the optimal model  $\mathbf{x}^{(0)} = \mathbf{0}$ , the covariance between  $A$  and  $B$  is defined as:

$$\text{cov}(A, B) = \frac{1}{M} \sum_{m=1}^M \left[ \left( A^{(m)} - \langle A \rangle \right) \left( B^{(m)} - \langle B \rangle \right) \right] = \langle AB \rangle - \langle A \rangle \langle B \rangle , \quad (12)$$

where  $A^{(m)} \equiv A(\mathbf{x}^{(m)})$  and “ $\langle \rangle$ ” denotes a statistical average. From the above definition the *correlation coefficient*—often called the Pearson product-moment correlation coefficient—now follows:

$$\rho(A, B) = \frac{\text{cov}(A, B)}{\sqrt{\text{var}(A) \text{var}(B)}} , \quad (13)$$

where the *variance* of  $A$  is simply given by  $\text{var}(A) \equiv \text{cov}(A, A)$ . Note that two observables are said to be fully correlated if  $\rho(A, B) = 1$ , fully anti-correlated if  $\rho(A, B) = -1$ , and uncorrelated if  $\rho(A, B) = 0$ . If one expands the deviation of both observables from their average value, then  $\text{cov}(A, B)$  may be written as

$$\text{cov}(A, B) = \sum_{i,j=1}^F \frac{\partial A}{\partial x_i} \left[ \frac{1}{M} \sum_{m=1}^M x_i^{(m)} x_j^{(m)} \right] \frac{\partial B}{\partial x_j} \equiv \sum_{i,j=1}^F \frac{\partial A}{\partial x_i} C_{ij} \frac{\partial B}{\partial x_j} , \quad (14)$$

where both derivatives are evaluated at the minimum ( $\mathbf{x}^{(0)} = \mathbf{0}$ ) and the *covariance matrix*  $C_{ij}$  has been introduced [26]. In order to continue, it is critical to decide how should the  $M$  points be generated. A particularly convenient choice

is to assume that these  $M$  points (or models) are distributed according to the quality measure  $\chi^2(\mathbf{x})$ . That is, we assume a probability distribution  $\phi(\mathbf{x})$  given by

$$\phi(\mathbf{x}) = \exp \left[ -\frac{1}{2} \Delta \chi^2(\mathbf{x}) \right] = \exp \left( -\frac{1}{2} \mathbf{x}^T \hat{\mathcal{M}} \mathbf{x} \right). \quad (15)$$

The covariance matrix may then be written as follows:

$$C_{ij} = \frac{\int x_i x_j \phi(\mathbf{x}) d\mathbf{x}}{\int \phi(\mathbf{x}) d\mathbf{x}} = \frac{1}{Z(0)} \left[ \frac{\partial^2 Z(\mathbf{J})}{\partial J_i \partial J_j} \right]_{\mathbf{J}=\mathbf{0}}, \quad (16)$$

where we have defined the “partition” function  $Z(\mathbf{J})$  as

$$Z(\mathbf{J}) = \int \phi(\mathbf{x}) e^{\mathbf{J} \cdot \mathbf{x}} d\mathbf{x} = \int \exp \left( -\frac{1}{2} \mathbf{x}^T \hat{\mathcal{M}} \mathbf{x} + \mathbf{J} \cdot \mathbf{x} \right) d\mathbf{x}. \quad (17)$$

The above gaussian integrals may be readily evaluated by completing the square. One obtains

$$Z(\mathbf{J}) = Z(0) \exp \left( \frac{1}{2} \mathbf{J}^T \hat{\mathcal{M}}^{-1} \mathbf{J} \right) \equiv Z(0) e^{W(\mathbf{J})}. \quad (18)$$

Hence, under the assumption that the model parameters are generated according to the  $\chi^2$ -measure, the covariance matrix becomes equal to the inverse of the matrix of second derivatives of  $\chi^2$ . That is,

$$C_{ij} = \frac{1}{Z(0)} \left[ \frac{\partial^2 Z(\mathbf{J})}{\partial J_i \partial J_j} \right]_{\mathbf{J}=\mathbf{0}} = \frac{\partial^2 W(\mathbf{J})}{\partial J_i \partial J_j} = (\mathcal{M}^{-1})_{ij} \quad (19)$$

Finally then, we arrive at a form for the covariance of two observables that is both simple and easy to compute:

$$\text{cov}(A, B) = \sum_{i,j=1}^F \frac{\partial A}{\partial x_i} (\hat{\mathcal{M}}^{-1})_{ij} \frac{\partial B}{\partial x_j} = \sum_{i=1}^F \frac{\partial A}{\partial \xi_i} \lambda_i^{-1} \frac{\partial B}{\partial \xi_i}. \quad (20)$$

The last term in the previous expression is particularly illuminating. Consider, for example, the case of a very soft direction in the  $\chi^2$ -measure, namely, an eigenvector of  $\hat{\mathcal{M}}$  (say  $\xi_i$ ) with a very small eigenvalue (say  $\lambda_i^{-1} \gg 1$ ). Such a situation routinely emerges in RMF models whenever two or more isovector parameters are included in the Lagrangian density but only masses and charge—not neutron—radii are used to define the  $\chi^2$ -measure. Having identified a soft direction, one could then search for an observable  $A$  (e.g., the neutron-skin thickness in  $^{208}\text{Pb}$ ) that is particularly sensitive to such a soft direction (as indicated by  $\partial A / \partial \xi_i \gg 1$ ). Adding such an observable to the  $\chi^2$ -measure will stiffen the formerly soft direction, thereby improving the predictive power of the model. Moreover, if  $A$  is difficult to measure, one could search for alternative observables that are strongly correlated to  $A$ . Although some of these notions have been heuristically implemented for some time, the statistical analysis discussed here provides a quantitative measure of the correlation between observables [5].

### III. RESULTS

In this section we provide two simple examples that illustrate the ideas presented in the previous sections. Here terms such as “*unique*” and “*predictive*” will be used to characterize a model. We regard a model as being unique if *all* the eigenvalues of  $\hat{\mathcal{M}}$  are large (i.e.,  $\lambda_i \gg 1$  for all  $i$ ). A model is predictive if it can successfully account for physical observables not included in the  $\chi^2$ -measure. Note that a model has been defined here as consisting of both an underlying Lagrangian density (or effective interaction) and a set of physical observables defining the  $\chi^2$ -measure.

#### A. Example 1: Linear Walecka Model

We start this section by discussing the linear Walecka model as an example of a model that is unique but not predictive. The Lagrangian density for this case is simple as it only contains two coupling constants [7, 12]. That is,

$$\mathcal{L}_{\text{int}} = g_s \bar{\psi} \psi \phi - g_v \bar{\psi} \gamma^\mu \psi V_\mu. \quad (21)$$

The Walecka model is perhaps the simplest model that can account—at the mean-field level—for the saturation of symmetric nuclear matter. Indeed, it is the saturation density and the energy per nucleon at saturation that are typically used to calibrate the two parameters of the model. To make this simple model slightly less trivial we determine the two parameters of the model by minimizing a quality measure  $\chi^2$  defined in terms of three “observables”: (i) the saturation density  $\rho_0$ , (ii) the energy per nucleon at saturation  $\varepsilon_0$ , and (iii) the effective Dirac mass  $M_0^*$ . Central values and uncertainties for these three quantities are given as follows:

$$\rho_0 = (0.155 \pm 0.01) \text{ fm}^{-3}, \quad (22a)$$

$$\varepsilon_0 = (-16 \pm 1) \text{ MeV}, \quad (22b)$$

$$M_0^* = (0.6 \pm 0.1) M. \quad (22c)$$

Using standard numerical techniques, a minimum value for the  $\chi^2$ -measure of  $\chi_0^2 = 0.34145$  is obtained at

$$g_s^2 = 93.62647, \quad (23a)$$

$$g_v^2 = 180.48347. \quad (23b)$$

Having computed the minimum value of the quality measure, we now examine its behavior around the minimum. This is implemented by diagonalizing the symmetric matrix of second derivatives  $\hat{\mathcal{M}}$  [see Eq. (10)]. The outcome of such a diagonalization procedure is the diagonal matrix of eigenvalues  $\hat{\mathcal{D}}$  and the orthogonal matrix of normalized eigenvectors  $\hat{\mathcal{A}}$ . That is,

$$\hat{\mathcal{D}} = \text{diag}(\lambda_1, \lambda_2) = \text{diag}(7.4399 \times 10^4, 8.3195 \times 10^1), \quad (24a)$$

$$\hat{\mathcal{A}} = \begin{pmatrix} \cos \theta & \sin \theta \\ -\sin \theta & \cos \theta \end{pmatrix} = \begin{pmatrix} 0.74691 & 0.66492 \\ -0.66492 & 0.74691 \end{pmatrix}. \quad (24b)$$

It is evident that both eigenvalues are very large. This indicates that both directions in parameter space are stiff and consequently the quality measure ( $\Delta\chi^2 = \lambda_1 \xi_1^2 + \lambda_2 \xi_2^2$ ) will deteriorate rapidly as one moves away from the  $\chi^2$ -minimum. Note that  $\lambda_1$  is significantly larger than  $\lambda_2$ ; this is to be expected. When probing the parameter landscape along the first direction (i.e.,  $\xi_2 = 0$ ) the scalar and vector coupling constants move “out-of-phase” (see the first column of the matrix  $\hat{\mathcal{A}}$ ). For example, the scalar attraction would get larger at the same time that the vector repulsion would get smaller. This would yield a significant increase in the binding energy per particle and consequently a drastic deterioration in the  $\chi^2$ -measure. Recall that large and *cancelling* scalar and vector potentials are the hallmark of relativistic mean-field models.

To quantify the extent by which the linear Walecka model is unique, we now proceed to compute the variance in the coupling constants using Eq. (20). We obtain

$$\sigma_s^2 = \left( \hat{\mathcal{M}}^{-1} \right)_{11} = \lambda_1^{-1} \cos^2 \theta + \lambda_2^{-1} \sin^2 \theta = 5.3217 \times 10^{-3}, \quad (25a)$$

$$\sigma_v^2 = \left( \hat{\mathcal{M}}^{-1} \right)_{22} = \lambda_1^{-1} \sin^2 \theta + \lambda_2^{-1} \cos^2 \theta = 6.7116 \times 10^{-3}. \quad (25b)$$

In turn, this translates into the following uncertainties in the optimal values of the coupling constants:

$$g_s^2 = 93.62647 (1 \pm \sigma_s) = 93.62647 \pm 6.83008, \quad (26a)$$

$$g_v^2 = 180.48347 (1 \pm \sigma_v) = 180.48347 \pm 14.78596. \quad (26b)$$

We conclude that the uncertainties in the model parameters—and thus in most of the predictions of the model—are of the order of 5-to-10 percent. In principle, the model uncertainties could be reduced by refining the experimental database [see Eq. (22)]. The great merit of the present statistical approach is that one may systematically explore the extent by which the experimental measurement must be refined in order to achieve the desired theoretical accuracy. Note that the theoretical uncertainties are dominated by the *smallest* eigenvalue of  $\hat{\mathcal{M}}$  [see Eq. (25)]. Thus, assessing the uniqueness of the model by varying each model-parameter individually (e.g, first  $g_s^2$  and then  $g_v^2$ ) is misleading and ill advised. It is misleading because in doing so the quality measure will in general be dominated by the *largest* eigenvalue [see Eq. (11)]. Yet it is the lowest eigenvalue that determines the uniqueness of the model.

Carrying out the covariance analysis further, we now proceed to compute correlation coefficients between model parameters and observables [see Eqs. (13) and (20)]. In estimating uncertainties in the model parameters one concentrates on the diagonal elements of the (inverse) matrix of second derivatives [see Eq. (25)]. Information on the

correlation between model parameters is, however, stored in the off-diagonal elements. For example, the correlation coefficient between  $g_s^2$  and  $g_v^2$  is given by

$$\rho(g_s^2, g_v^2) = \frac{(\hat{\mathcal{M}}^{-1})_{12}}{\sqrt{(\hat{\mathcal{M}}^{-1})_{11} (\hat{\mathcal{M}}^{-1})_{22}}} = 0.9977. \quad (27)$$

The strong (positive) correlation between  $g_s^2$  and  $g_v^2$  is easily understood. Given that configurations in parameter space are distributed according to the  $\chi^2$ -measure, model parameters in which  $g_s^2$  and  $g_v^2$  move out-of-phase are strongly suppressed, as they are controlled by the largest eigenvalue  $\lambda_1$ . As a result, an overwhelming number of configurations are generated with  $g_s^2$  and  $g_v^2$  moving in phase, thereby leading to a large positive correlation. Correlation coefficients between various isoscalar observables have been tabulated in Table I. Given that the correlation coefficients are sensitive to the first derivatives of the observables along all (eigen)directions [see Eq. (20)], we have listed them for completeness in Table II. We observe that all observables display a much larger sensitivity to the stiff direction than to the soft one. This could (and does) lead to sensitive cancellations since the large derivatives compensate for the small value of  $\lambda_1^{-1}$ . Indeed, the correlation between the saturation density and the binding energy at saturation is very small. On the other hand, the incompressibility coefficient appears to be strongly correlated to the binding energy. This behavior is also displayed in graphical form in Fig. 1 where predictions for the various observables were generated with model parameters distributed according to  $\phi(\mathbf{x})$  [see Eq. (15)]. Note that the *covariance ellipsoids* in Fig. 1 were generated by selecting those model parameters that satisfy  $\Delta\chi^2 \leq 1$ .

	$\varepsilon_0$	$\rho_0$	$K_0$	$M_0^*$
$\varepsilon_0$	+1.0000	-0.0036	-0.9998	+0.8867
$\rho_0$	-0.0036	+1.0000	-0.0174	+0.4591
$K_0$	-0.9998	-0.0174	+1.0000	+0.8962
$M_0^*$	+0.8867	+0.4591	+0.8962	+1.0000

TABLE I: Correlation coefficients between isoscalar observables in the linear Walecka model.

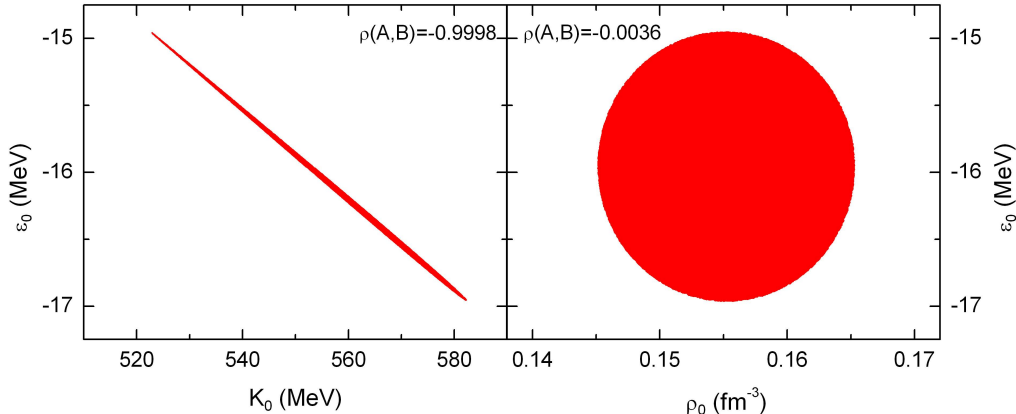


FIG. 1: (Color online) Predictions from the linear Walecka models for the saturation density, binding energy, and incompressibility coefficient at saturation. Model parameters were generated according to the distribution  $\exp(-\Delta\chi^2/2)$ . Both of the covariance ellipsoids were generated by limiting the models to the region  $\Delta\chi^2 \leq 1$ .

Based on the previous statistical analysis it appears that the linear Walecka model is unique (at least at the 5–10% level). But is the linear Walecka model predictive? To test the predictability of the model we focus on two physical observables that were not included in the  $\chi^2$ -measure, namely, the incompressibility coefficient  $K_0$  and the symmetry energy  $J$ . We obtain—with properly computed theoretical errors—the following results:

$$K_0 = (552.537 \pm 29.655) \text{ MeV}, \quad (28a)$$

$$J = (19.775 \pm 0.683) \text{ MeV}. \quad (28b)$$



	$\partial\xi_1$	$\partial\xi_2$
$\partial\varepsilon_0$	$-1.6698 \times 10^1$	$-1.1716 \times 10^{-1}$
$\partial\rho_0$	3.6619	$-5.7333 \times 10^{-1}$
$\partial K_0$	$1.4261 \times 10^1$	$1.1055 \times 10^{-1}$
$\partial M_0^*$	-3.2349	$-8.8817 \times 10^{-2}$

TABLE II: First derivatives of the *scaled* observables (i.e., observable scaled to its value at the  $\chi^2$ -minimum) as a function of  $\xi_1$  and  $\xi_2$  evaluated at the  $\chi^2$ -minimum; see Eq. (20).

Both predictions, even after theoretical errors have been incorporated, differ significantly from the presently acceptable values of  $K_0 \approx (240 \pm 20)$  MeV and  $J \approx (32 \pm 2)$  MeV. This conclusion should hardly come as a surprise. After all, the predominant role played by the model parameters  $\kappa$  and  $\lambda$  in softening the incompressibility coefficient and  $g_\rho$  in stiffening the symmetry energy have been known for a long time. What is relevant from the present statistical analysis is that we have established quantitatively that the linear Walecka model fails because its prediction for  $K_0$  differs from the experimental value by more than 10 standard deviations. We must then conclude that whereas the linear Walecka is (fairly) unique, it is not predictive. We now proceed to discuss a particular extension of the Walecka model that is highly predictive but not unique: the non-linear FSUGold model.

### B. Example 2: Non-linear FSUGold Model

Modern relativistic models of nuclear structure have evolved significantly since the early days of the linear Walecka model. In the present example we focus on the FSUGold parameter set [18] that is defined by an interacting Lagrangian density of the following form:

$$\mathcal{L}_{\text{int}} = \bar{\psi} \left[ g_s \phi - \left( g_v V_\mu + \frac{g_\rho}{2} \boldsymbol{\tau} \cdot \mathbf{b}_\mu + \frac{e}{2} (1 + \tau_3) A_\mu \right) \gamma^\mu \right] \psi - \frac{\kappa}{3!} \Phi^3 - \frac{\lambda}{4!} \Phi^4 + \frac{\zeta}{4!} \left( W_\mu W^\mu \right)^2 + \Lambda_v \left( W_\nu W^\nu \right) \left( \mathbf{B}_\mu \cdot \mathbf{B}^\mu \right). \quad (29)$$

Modifications to the linear Walecka model are motivated by the availability of an ever increasing database of high-quality data. For example, the two non-linear scalar terms  $\kappa$  and  $\lambda$  induce a significant softening of the compression modulus of nuclear matter relative to the original Walecka model [7, 12, 14]. This is demanded by measurement of the giant monopole resonance in medium to heavy nuclei [27]. Further, omega-meson self-interactions, as described by the parameter  $\zeta$ , also serve to soften the equation of state of symmetric nuclear matter but at much higher densities. Indeed, by tuning the value of  $\zeta$  it is possible to produce maximum neutron star masses that differ by almost one solar mass while maintaining the saturation properties of nuclear matter intact [9]. Such a softening appears consistent with the dynamics of high-density matter as probed by energetic heavy-ion collisions [28]. Finally,  $\Lambda_v$  induces isoscalar-isovector mixing and is responsible for modifying the poorly-constrained density dependence of the symmetry energy [17, 29]. In particular, a softening of the symmetry energy induced by  $\Lambda_v$  appears consistent with the distribution of both isoscalar monopole and isovector dipole strength in medium to heavy nuclei [18, 30, 31]. In summary, FSUGold is a fairly successful RMF model that has been validated against theoretical, experimental, and observational constraints [19]. Note that as additional laboratory and observational data become available (notably the recent report of a 2-solar mass neutron star [32]) refinements to the model may be required [20]. For now, however, we will be content with using the FSUGold model to study the small oscillations around the minimum.

As mentioned earlier, a model should be understood as a combination of an interacting Lagrangian density and a quality measure. We define the  $\chi^2$ -measure in terms of the following set of observables generated directly from the FSUGold parameter set:

$$\rho_0 = 0.1484 \text{ fm}^{-3}, \quad (30a)$$

$$\varepsilon_0 = -16.30 \text{ MeV}, \quad (30b)$$

$$\varepsilon(2\rho_0) = -5.887 \text{ MeV}, \quad (30c)$$

$$K_0 = 230.0 \text{ MeV}, \quad (30d)$$

$$M_0^* = 0.6100 M, \quad (30e)$$

$$\tilde{J} = 26.00 \text{ MeV}, \quad (30f)$$

$$L = 60.52 \text{ MeV}, \quad (30g)$$

$$M_{\text{max}} = 1.722 M_\odot. \quad (30h)$$

Note that in all cases a 2% uncertainty is attached to all observables—except in the case of the slope of the symmetry energy  $L$  where the significant larger value of 20% is assumed. This reflects our poor understanding of the density

dependence of the symmetry energy. Also note that  $\tilde{J}$  represents the value of the symmetry energy at a sub-saturation density of  $\rho \approx 0.1 \text{ fm}^{-3}$ —a density at which the theoretical uncertainties are minimized [33]. Finally, notwithstanding the Demorest *et al.* result [32], the maximum neutron star mass is fixed at  $M_{\text{max}} = 1.722 M_{\odot}$ . Given that a theoretical model is used to generate the various observables, a much larger database could be used to define the  $\chi^2$ -measure, if desired. By construction, a very small value for the  $\chi^2$ -measure is obtained at the FSUGold minimum. We now proceed to explore the wealth of information available as one studies deviations around this minimum value. As in the previous section, the symmetric matrix of second derivatives  $\hat{\mathcal{M}}$  (now a  $7 \times 7$  matrix) may be diagonalized by means of an orthogonal transformation. The diagonal matrix of eigenvalues  $\hat{\mathcal{D}}$  and the matrix of eigenvectors  $\hat{\mathcal{A}}$  are given by

$$\hat{\mathcal{D}} = \text{diag}(1.2826 \times 10^6, 1.5305 \times 10^4, 4.2472 \times 10^2, 3.2113 \times 10^2, 1.2692 \times 10^2, 6.9619, 3.7690), \quad (31a)$$

$$\hat{\mathcal{A}} = \begin{pmatrix} -7.4967 \times 10^{-1} & -2.3685 \times 10^{-1} & 3.0853 \times 10^{-1} & 1.2931 \times 10^{-1} & -5.1254 \times 10^{-1} & -8.5089 \times 10^{-2} & 6.8417 \times 10^{-3} \\ 6.5682 \times 10^{-1} & -1.5751 \times 10^{-1} & 3.6654 \times 10^{-1} & 1.6504 \times 10^{-1} & -6.0281 \times 10^{-1} & -1.3685 \times 10^{-1} & 8.5353 \times 10^{-3} \\ -1.5331 \times 10^{-4} & 3.1315 \times 10^{-3} & -7.0050 \times 10^{-1} & 6.8701 \times 10^{-2} & -3.9206 \times 10^{-1} & -3.3843 \times 10^{-2} & 5.9137 \times 10^{-1} \\ 3.8535 \times 10^{-2} & -2.8770 \times 10^{-1} & -2.4254 \times 10^{-2} & 4.7416 \times 10^{-1} & 4.3796 \times 10^{-2} & 8.2968 \times 10^{-1} & -5.7643 \times 10^{-3} \\ 3.9417 \times 10^{-2} & -6.8525 \times 10^{-1} & -1.3772 \times 10^{-1} & 3.8776 \times 10^{-1} & 3.5428 \times 10^{-1} & -4.8376 \times 10^{-1} & 2.6431 \times 10^{-3} \\ -5.9458 \times 10^{-2} & 6.0558 \times 10^{-1} & 5.4897 \times 10^{-2} & 7.5689 \times 10^{-1} & 6.8021 \times 10^{-2} & -2.2175 \times 10^{-1} & 6.2795 \times 10^{-3} \\ 1.2995 \times 10^{-4} & -3.1465 \times 10^{-3} & 5.0714 \times 10^{-1} & -5.7010 \times 10^{-2} & 2.9691 \times 10^{-1} & 3.6238 \times 10^{-2} & 8.0628 \times 10^{-1} \end{pmatrix}. \quad (31b)$$

Note that the scaled parameters of the model are associated to the original coupling constants as follows:

$$\{x_1, x_2, x_3, x_4, x_5, x_6, x_7\} \rightarrow \{g_s^2, g_v^2, g_\rho^2, \kappa, \lambda, \zeta, \Lambda_v\}. \quad (32)$$

We observe that the stiffest direction is dominated by two isoscalar parameters and represents—as in the case of the linear Walecka model—an out-of-phase oscillation between the scalar attraction and the vector repulsion. Given that in RMF models the cancellation between the scalar attraction and the vector repulsion is so delicate, any out-of-phase motion yields a significant change in the binding energy per nucleon and a correspondingly dramatic increase in the quality measure. The second stiffest direction also involves exclusively isoscalar parameters and is dominated by the quartic scalar ( $\lambda$ ) and vector ( $\zeta$ ) couplings—and to a lesser extent by the cubic term ( $\kappa$ ). This linear combination of parameters is largely constrained by the incompressibility coefficient  $K_0$  and the maximum neutron-star mass  $M_{\text{max}}$ . Although the determination of the maximum neutron-star mass to a 2% accuracy presents a significant observational challenge, our statistical analysis suggests that such a determination would strongly constrain the equation of state from saturation density up to neutron-star densities. The third stiffest direction (with still a fairly large eigenvalue of  $\lambda_3 \approx 425$ ) is dominated by the two isovector parameters  $g_\rho^2$  and  $\Lambda_v$ . For this particular “mode” both parameters oscillate out of phase. This behavior can be readily understood by recalling the expression for the symmetry energy [29]:

$$E_{\text{sym}}(\rho) = \frac{k_F^2}{6E_F^*} + \frac{g_\rho^2 \rho}{8m_\rho^{*2}}, \quad \left(m_\rho^{*2} \equiv m_\rho^2 + 2\Lambda_v g_\rho^2 W_0^2\right). \quad (33)$$

In order for the symmetry energy  $\tilde{J}$  to remain fixed, then both  $g_\rho^2$  and  $\Lambda_v$  must move in phase. If they move out of phase, then the symmetry energy can not be kept at this value and the quality measure deteriorates. By the same token, the in-phase motion of  $g_\rho^2$  and  $\Lambda_v$  is very poorly constrained—as evinced by the last and softest direction. And it is only because the slope of the symmetry energy  $L$  was assumed to be somehow constrained (at the 20% level) that a positive eigenvalue was even obtained. Note that one of the main goals of the successfully commissioned Lead Radius experiment (PREx) at the Jefferson Laboratory is to constrain the density dependence of the symmetry energy (*i.e.*,  $L$ ) by accurately measuring the neutron radius of  $^{208}\text{Pb}$  [34, 35]. The next to last eigenvalue ( $\lambda_6 \approx 7$ ) is also relatively small. This suggest that the out-of-phase motion of the two non-linear scalar couplings ( $\kappa$  and  $\lambda$ ) is poorly constrained by the nuclear-matter observables defining the quality measure. Perhaps supplementing the quality measure with finite-nuclei observables will help ameliorate this problem. Work along these lines is currently in progress.

We now proceed to estimate theoretical uncertainties as well as to compute correlation coefficients for both the model parameters and the physical observables. We start by computing theoretical uncertainties (*i.e.*, variances) for the model parameters. These are given by [see Eq. (20)]

$$\sigma_i^2 = \left(\hat{\mathcal{M}}^{-1}\right)_{ii} = \left(\hat{\mathcal{A}}\hat{\mathcal{D}}^{-1}\hat{\mathcal{A}}^T\right)_{ii} = \sum_{j=1}^7 \mathcal{A}_{ij}^2 \lambda_j^{-1}, \quad (34)$$

and result in the following theoretical uncertainties for the model parameters:

$$g_s^2 = 112.19955 \pm 6.54468 \text{ [5.833\%]}, \quad (35a)$$

$$g_v^2 = 204.54694 \pm 15.81183 \text{ [7.730\%]}, \quad (35b)$$

$$g_\rho^2 = 138.47011 \pm 42.75427 \text{ [30.876\%]}, \quad (35c)$$

$$\kappa = 1.42033 \pm 0.44827 \text{ [31.561\%]}, \quad (35d)$$

$$\lambda = 0.02376 \pm 0.00445 \text{ [18.748\%]}, \quad (35e)$$

$$\zeta = 0.06000 \pm 0.0057 \text{ [9.447\%]}, \quad (35f)$$

$$\Lambda_v = 0.03000 \pm 0.01251 \text{ [41.711\%]}. \quad (35g)$$

We observe that three out of the five isoscalar parameters, namely,  $g_s^2$ ,  $g_v^2$ , and  $\zeta$ , are relatively well constrained (at the  $\lesssim 10\%$  level). Whereas  $g_s^2$  and  $g_v^2$  are well determined by the saturation properties of symmetric nuclear matter, it is the maximum neutron-star mass that constrains  $\zeta$ . Yet the remaining two isoscalar parameters ( $\kappa$  and  $\lambda$ ) are poorly determined. This is particularly true in the case of  $\kappa$  which displays a large ( $\approx 30\%$ ) uncertainty. As alluded earlier, these large uncertainties develop because the out-of-phase motion of  $\kappa$  and  $\lambda$ —as controlled by the relatively soft sixth eigenvector—is poorly constrained. Given that the in-phase motion of the two isovector parameters ( $g_\rho^2$  and  $\Lambda_v$ ) is controlled by the softest of eigenvectors, the theoretical uncertainties in these parameters is also fairly large ( $\approx 30\%$  and  $\approx 40\%$ , respectively). However, whereas the reason for the latter is associated with the large error bars assigned to  $L$ , we are unaware at this time on how to better constrain  $\kappa$  and  $\lambda$ . Perhaps supplementing the quality measure with information on various nuclear compressional modes may help resolve this issue. Plans to do so in the near future are under consideration.

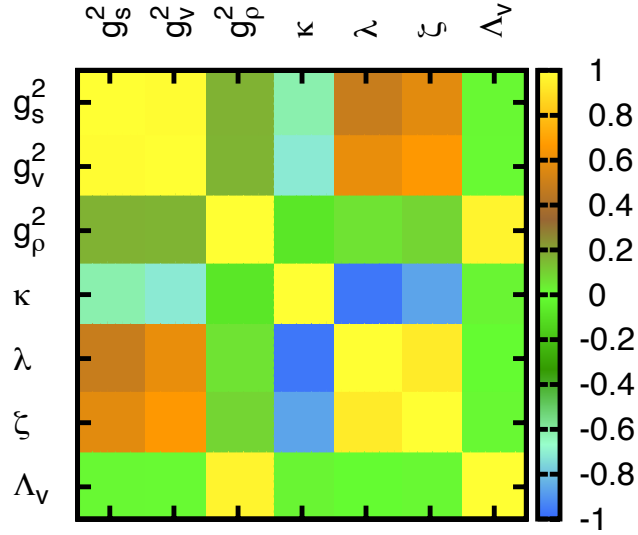


FIG. 2: (Color online) Color-coded plot of the 21 independent correlation coefficients between the 7 model parameters of the FSUGold effective interaction.

We have computed correlation coefficients between all 21 distinct pairs of model parameters and have displayed them in graphical (color-coded) form in Fig. 2. As depicted in the figure, the strongest correlations are between  $g_s^2$  and  $g_v^2$  (0.988),  $g_\rho^2$  and  $\Lambda_v$  (0.967), and  $\kappa$  and  $\lambda$  (-0.962). As alluded in the case of the simpler linear Walecka model, the correlations are dominated by the *softest directions*; in this case the sixth and seventh eigenvectors. Given that for these two eigenvectors  $g_s^2$  and  $g_v^2$  as well as  $g_\rho^2$  and  $\Lambda_v$  move in phase whereas  $\kappa$  and  $\lambda$  move out of phase, the observed correlations ensue. In other words, the three largest eigenvalues strongly suppress the generation of model parameters with  $g_s^2$  and  $g_v^2$  moving out of phase,  $\kappa$  and  $\lambda$  in phase, and  $g_\rho^2$  and  $\Lambda_v$  out of phase, respectively. Note then, that the distribution of isovector parameters  $g_\rho^2$  and  $\Lambda_v$  is generated in such a way that the symmetry energy at sub-saturation density  $\tilde{J}$  remains fixed at 26 MeV (at least within a 2% uncertainty). This quantitative fact validates

our heuristic approach—already employed numerous times—to correlate isovector observables (see Refs. [6, 36, 37] and references therein).

We now extend the covariance analysis to the case of physical observables. To do so, we must supply the relevant “matrix” of first derivatives [see Eq. (20)]. For completeness we list the first derivatives in tabular form in Table III. Note that in the case of the model parameters the corresponding matrix of first derivatives is the matrix of eigenvectors  $\hat{\mathcal{A}}$ . The derivatives encapsulate the sensitivity of the various observables to changes along the different eigenvectors. For example, whereas isoscalar observables (such as  $\varepsilon_0, \rho_0, K_0$ ) are insensitive to changes along the mostly isovector seventh eigenvector, both  $L$  and the neutron-skin thickness of  $^{208}\text{Pb}$ ,  $R_n - R_p$ , display a fairly large sensitivity.

	$\partial\xi_1$	$\partial\xi_2$	$\partial\xi_3$	$\partial\xi_4$	$\partial\xi_5$	$\partial\xi_6$	$\partial\xi_7$
$\partial\varepsilon_0$	$1.0551 \times 10^{+1}$	$-7.1882 \times 10^{-1}$	$-2.9433 \times 10^{-2}$	$4.9029 \times 10^{-2}$	$5.1626 \times 10^{-2}$	$-1.7025 \times 10^{-2}$	$-7.7009 \times 10^{-4}$
$\partial\rho_0$	$-2.2472$	$1.3904$	$-9.8868 \times 10^{-4}$	$2.2220 \times 10^{-1}$	$5.3440 \times 10^{-2}$	$1.8998 \times 10^{-2}$	$1.5875 \times 10^{-3}$
$\partial K_0$	$-7.4792$	$1.3890$	$-3.6799 \times 10^{-2}$	$-1.8808 \times 10^{-1}$	$4.8215 \times 10^{-2}$	$-2.1691 \times 10^{-2}$	$-3.0813 \times 10^{-4}$
$\partial M^*$	$1.1505$	$-5.5581 \times 10^{-1}$	$-1.0614 \times 10^{-1}$	$-8.3170 \times 10^{-2}$	$1.6492 \times 10^{-1}$	$1.2614 \times 10^{-2}$	$-2.7701 \times 10^{-3}$
$\partial\tilde{J}$	$-2.7862 \times 10^{-1}$	$6.5586 \times 10^{-2}$	$-3.9136 \times 10^{-1}$	$2.5698 \times 10^{-2}$	$-6.8299 \times 10^{-2}$	$6.0862 \times 10^{-4}$	$6.2323 \times 10^{-4}$
$\partial J$	$-1.6811$	$9.4897 \times 10^{-1}$	$-3.2446 \times 10^{-1}$	$1.7826 \times 10^{-1}$	$-3.6792 \times 10^{-2}$	$6.2151 \times 10^{-3}$	$-8.4827 \times 10^{-2}$
$\partial L$	$-1.8759$	$1.1812$	$1.5849 \times 10^{-2}$	$2.6611 \times 10^{-1}$	$-1.0180 \times 10^{-1}$	$-2.2526 \times 10^{-2}$	$-3.8593 \times 10^{-1}$
$\partial(R_n - R_p)$	$7.0224$	$9.6188 \times 10^{-2}$	$-2.3362 \times 10^{-1}$	$1.9804 \times 10^{-1}$	$-2.5651 \times 10^{-2}$	$-1.9368 \times 10^{-2}$	$-3.4167 \times 10^{-1}$
$\partial R_{1.0}$	$9.9947 \times 10^{-1}$	$-3.1989 \times 10^{-1}$	$-1.6534 \times 10^{-2}$	$-6.5939 \times 10^{-2}$	$-4.5197 \times 10^{-2}$	$-4.5964 \times 10^{-3}$	$-3.9800 \times 10^{-2}$
$\partial R_{1.4}$	$5.0300 \times 10^{-1}$	$-3.0884 \times 10^{-1}$	$9.3778 \times 10^{-3}$	$-1.1119 \times 10^{-1}$	$-6.3792 \times 10^{-2}$	$3.1016 \times 10^{-3}$	$-2.6571 \times 10^{-2}$
$\partial M_{\text{max}}$	$-2.7675 \times 10^{-1}$	$-1.4882 \times 10^{-1}$	$3.1173 \times 10^{-2}$	$-1.6394 \times 10^{-1}$	$-6.8790 \times 10^{-2}$	$3.4817 \times 10^{-2}$	$-2.4367 \times 10^{-3}$

TABLE III: First derivatives of the *scaled* observables (i.e., observable scaled to its value at the  $\chi^2$ -minimum) as a function of  $\xi_i$  at the  $\chi^2$ -minimum; see Eq. (20).

Given the enormous interest in constraining the density dependence of the symmetry energy, we estimate theoretical uncertainties on three—mostly isovector—observables. These are the symmetry energy at saturation density  $J$ , the neutron-skin thickness of  $^{208}\text{Pb}$ , and the radius ( $R_{1.4}$ ) of a  $M = 1.4M_\odot$  neutron star. Recall that it was  $\tilde{J}$  (not  $J$ ) that was included in the definition of the quality measure. We obtain,

$$J = (32.593 \pm 1.574) \text{ MeV} \quad [4.830\%], \quad (36a)$$

$$R_n - R_p = (0.207 \pm 0.037) \text{ fm} \quad [17.698\%], \quad (36b)$$

$$R_{1.4} = (11.890 \pm 0.194) \text{ km} \quad [1.631\%]. \quad (36c)$$

We now comment on each of these cases individually. Before we do so, however, note that correlation coefficients for 11 observables (i.e., 55 independent pairs) are depicted in a color-coded format in Fig. 3. First, the central value of  $J$  along with its theoretical uncertainty may be easily understood by invoking a first-order expansion for the symmetry energy  $\tilde{J}$  at sub-saturation density ( $\tilde{\rho}_0 \approx 0.103 \text{ fm}^{-3}$ ) in terms of  $J$  and  $L$  [38]. That is,

$$J = \tilde{J} + xL + \dots \approx (32.208 \pm 1.346) \text{ MeV}, \quad x = \frac{1}{3} \left( 1 - \frac{\tilde{\rho}_0}{\rho_0} \right) \approx 0.103, \quad (37)$$

where the errors were added in quadrature. So although  $J$  is strongly correlated to  $L$  (with a correlation coefficient of 0.922) the error in the former is significantly smaller than the latter because of the small value of  $x$ . Second, for the neutron-skin thickness of  $^{208}\text{Pb}$  we find a theoretical error comparable to the one assumed for  $L$  and a correlation coefficient between the two observables of almost one (0.995). Such a strong correlation is consistent with two recent studies that employ a large number of accurately-calibrated relativistic and non-relativistic interactions to uncover the correlation [39, 40]. Also consistent with these studies, specifically with Ref. [40], is the fact that the proposed 1% measurement of the neutron radius of  $^{208}\text{Pb}$  by the PREx collaboration [34, 35] may not be able to place a significant constrain on  $L$ . For example, our covariance analysis suggests that the 20% uncertainty assumed for  $L$  translates into a theoretical error in the neutron skin of 0.037 fm—or about a 0.7% uncertainty in the neutron radius of  $^{208}\text{Pb}$ . Conversely, if  $L$  is to be determined to within 10% (i.e.,  $L \approx 60 \pm 6 \text{ MeV}$ ) then the neutron skin must be constrained to about 0.018 fm so the neutron radius must be measured with close to a 0.3% accuracy—a fairly daunting task. Finally, we obtain a very small theoretical uncertainty for the radius of a 1.4 solar-mass neutron star and a correlation coefficient between  $L$  and  $R_{1.4}$  (or  $R_n - R_p$  and  $R_{1.4}$ ) of 0.811. Although the radius of the neutron star is sensitive to the density dependence of the symmetry energy [41],  $R_{1.4}$  can not be uniquely constrained by a measurement of  $R_n - R_p$  because whereas the latter depends on the symmetry energy at (or below) saturation density, the former is also sensitive to the equation of state at higher densities [29]. Note that a far better correlation coefficient of

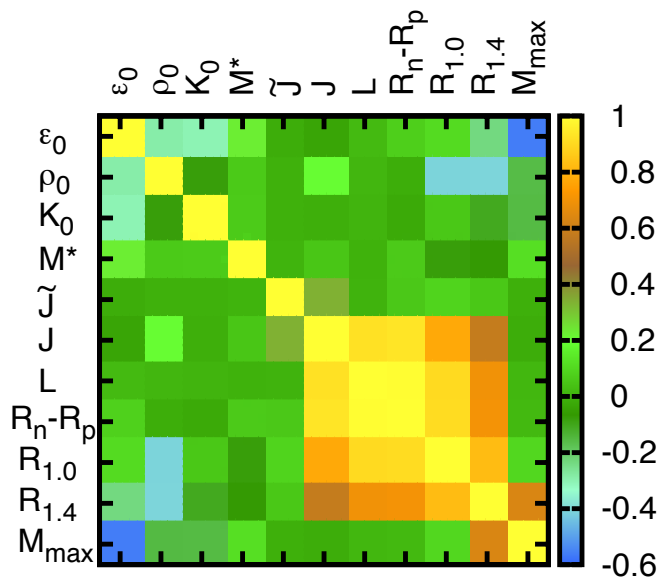


FIG. 3: (Color online) Color-coded plot of the 55 independent correlation coefficients between 11 physical observables as computed with the FSUGold effective interaction.

0.942 is obtained between  $L$  and the radius of a 1.0 solar-mass neutron star. Regardless (with all things being equal) knowledge of the slope of the symmetry energy to a 20% accuracy significantly constrains the stellar radius.

#### IV. CONCLUSIONS

The demand for theoretical predictions that include meaningful and reliable uncertainties is increasing. Such a sentiment has been articulated in a recent publication by the editors of the Physical Review A [2]. The need to quantify model uncertainties in an area such as theoretical nuclear physics is particularly urgent as models that are fitted to experimental data are then used to extrapolate to the extremes of temperature, density, isospin asymmetry, and angular momentum. Inspired by some of the central ideas developed in Ref. [5], a systematic statistical approach was applied to a class of relativistic mean-field models. The aim of this statistical analysis was twofold. First, to attach meaningful and reliable theoretical uncertainties to both the model parameters as well as to the predicted observables. Second, to quantify the degree of correlation between physical observables.

Modern relativistic mean-field models have evolved considerably since the early days of the linear Walecka model. Based on certain shortcomings of the Walecka model—most notably the inability to reproduce the incompressibility coefficient of symmetric nuclear matter—the Lagrangian density was augmented by non-linear cubic and quartic scalar-meson terms. However, based on modern effective-field-theory tenets, such as naturalness and power counting, a consistent Lagrangian density should include all terms up to fourth order in the meson fields. But in doing so, how should one constrain the large number of model parameters? In principle, one should follow the standard protocol of determining all model parameters through a  $\chi^2$ -minimization procedure. In practice, however, many successful theoretical approaches arbitrarily set some of the model parameters to zero. The argument behind this fairly ad-hoc procedure is that the full set of parameters is poorly determined by existing data, so ignoring a subset model parameters does not compromise the quality of the fit.

A covariance analysis such as the one implemented here should be able to clarify in a quantitative fashion the precise meaning of a “poorly determined set of parameters”. To do so, one should focus—not on the minimum of the  $\chi^2$ -measure but rather—on its behavior around the minimum. As in any small-oscillations problem, the deviations around the minimum are controlled by a symmetric matrix of second derivatives that may be used to extract theoretical error bars and to compute correlation coefficients among physical observables. However, to access the wealth of information available in the covariance analysis we took it a step further and diagonalized the matrix of second derivatives. Upon diagonalization, the deviations of the  $\chi^2$ -measure from the minimum are parametrized in terms of a collection of “uncoupled harmonic oscillators”. By doing so, one could readily identify stiff and soft modes in parameter space,

namely, eigenvectors characterized by either large or small eigenvalues, respectively.

We now summarize some of the most important lessons learned. First, a stiff direction represents a particular linear combination of model parameters that is well constrained by the set of physical observables included in the  $\chi^2$ -measure. By the same token, a soft direction suggests that additional physical observables are required to further constrain the model. Second, given that model parameters around the minimum are distributed according to the  $\chi^2$ -measure, the soft directions dominate the correlation analysis. Finally, testing whether a model is well constrained by individually varying its parameters—rather than by varying them coherently as suggested by the structure of the eigenvectors—may be misleading. To illustrate these findings we used two relatively simple, yet illuminating, examples: (a) the linear Walecka model and (b) the FSUGold parametrization. Note that ultimately we aim to implement the covariance analysis with a  $\chi^2$ -measure defined by a consistent Lagrangian density.

A particularly clear example of a stiff direction was represented by the out-of-phase motion of the scalar  $g_s$  and vector  $g_v$  coupling constants in the linear Walecka model. Indeed, increasing the scalar attraction while at the same time reducing the vector repulsion leads to a significant increase in the binding energy per nucleon and, thus, in a significant deterioration of the  $\chi^2$ -measure. The in-phase motion of  $g_s$  and  $g_v$ , however, is not as well constrained (the ratio of the two eigenvalues is about 1000). Therefore, configurations in parameter space generated by the  $\chi^2$ -measure were dominated by pairs of coupling constants that were in phase, thereby resulting in a correlation coefficient between  $g_s$  and  $g_v$  that was, as expected, large and positive. Note, however, that if  $g_s$  and  $g_v$  were varied individually, one would erroneously conclude that the model is much better constrained than it really is—since changes in the  $\chi^2$ -measure would be dominated by the largest eigenvalue.

In our second example we considered the accurately-calibrated FSUGold interaction with an isovector interaction determined by two parameters ( $g_\rho$  and  $\Lambda_v$ ). We found the out-of-phase motion of  $g_\rho$  and  $\Lambda_v$  to be strongly constrained by the value of the symmetry energy at a density of about 0.1 fm. However, our poor knowledge of the density dependence of the symmetry energy left the in-phase motion of  $g_v$  and  $\Lambda_v$  largely unconstrained. Effectively then, correlations in the isovector sector were induced by the in-phase motion of  $g_\rho$  and  $\Lambda_v$ —subject to the constraint that the symmetry energy at  $\rho \approx 0.1$  fm remains intact. This procedure validates the heuristic approach that we have used for some time to estimate correlations among isovector observables. Yet a benefit of the present analysis is that one can precisely quantify the theoretical errors as well as the correlation among observables. For example, we concluded that if the slope of the symmetry energy is to be determined with a 10% uncertainty, then the neutron-skin thickness of  $^{208}\text{Pb}$  should be measured with a 0.3% accuracy. This more stringent limit seems to agree with the conclusions of Ref. [40].

In the future we aim to apply the covariance analysis discussed here to the construction of a relativistic density functional that will include all terms up to fourth order in the meson fields. Moreover, we plan to calibrate the  $\chi^2$ -measure using various properties of finite nuclei and neutron stars. In addition, we reiterate a point made in Ref. [5] that the methodology used in this work should be applicable to any problem where model parameters are determined from optimizing a quality measure.

### Acknowledgments

We thank Profs. W. Nazarewicz and P.-G. Reinhard for many useful conversations. We also thank Prof. M. Riley for calling our attention to Ref. [2]. This work was supported in part by the United States Department of Energy under grant DE-FG05-92ER40750.

- 
- [1] *Building a universal nuclear energy density functional*, (UNEDF Collaboration), URL <http://unedf.org>.
  - [2] The Editors, Phys. Rev. A **83**, 040001 (2011).
  - [3] W. Kohn, Rev. Mod. Phys. **71**, 1253 (1999).
  - [4] W. Kohn and L. J. Sham, Phys. Rev. **140**, A1133 (1965).
  - [5] P.-G. Reinhard and W. Nazarewicz, Phys. Rev. **C81**, 051303 (2010).
  - [6] J. Piekarewicz, Phys. Rev. **C83**, 034319 (2011).
  - [7] B. D. Serot and J. D. Walecka, Adv. Nucl. Phys. **16**, 1 (1986).
  - [8] B. D. Serot and J. D. Walecka, Int. J. Mod. Phys. **E6**, 515 (1997).
  - [9] H. Mueller and B. D. Serot, Nucl. Phys. **A606**, 508 (1996).
  - [10] B. Liu, V. Greco, V. Baran, M. Colonna, and M. Di Toro, Phys. Rev. **C65**, 045201 (2002).
  - [11] V. Baran, M. Colonna, V. Greco, and M. Di Toro, Phys. Rept. **410**, 335 (2005).
  - [12] J. D. Walecka, Annals Phys. **83**, 491 (1974).
  - [13] C. J. Horowitz and B. D. Serot, Nucl. Phys. **A368**, 503 (1981).

- [14] J. Boguta and A. R. Bodmer, Nucl. Phys. **A292**, 413 (1977).
- [15] G. A. Lalazissis, J. Konig, and P. Ring, Phys. Rev. **C55**, 540 (1997).
- [16] G. A. Lalazissis, S. Raman, and P. Ring, At. Data Nucl. Data Tables **71**, 1 (1999).
- [17] C. J. Horowitz and J. Piekarewicz, Phys. Rev. Lett. **86**, 5647 (2001).
- [18] B. G. Todd-Rutel and J. Piekarewicz, Phys. Rev. Lett. **95**, 122501 (2005).
- [19] J. Piekarewicz, Phys. Rev. **C76**, 064310 (2007).
- [20] F. J. Fattoyev, C. J. Horowitz, J. Piekarewicz, and G. Shen, Phys. Rev. **C82**, 055803 (2010).
- [21] R. J. Furnstahl, B. D. Serot, and H.-B. Tang, Nucl. Phys. **A615**, 441 (1997).
- [22] R. J. Furnstahl, B. D. Serot, and H.-B. Tang, Nucl. Phys. **A618**, 446 (1997).
- [23] B. Agrawal, Phys. Rev. **C81**, 034323 (2010).
- [24] R. J. Furnstahl, B. D. Serot, and H.-B. Tang, Nucl. Phys. **A598**, 539 (1996).
- [25] A. Tamii et al., Phys. Rev. Lett. **107**, 062502 (2011).
- [26] S. Brandt, *Data Analysis: Statistical and Computational Methods for Scientists and Engineers* (Springer, New York, 1999), 3rd ed.
- [27] D. H. Youngblood, H. L. Clark, and Y.-W. Lui, Phys. Rev. Lett. **82**, 691 (1999).
- [28] P. Danielewicz, R. Lacey, and W. G. Lynch, Science **298**, 1592 (2002).
- [29] C. J. Horowitz and J. Piekarewicz, Phys. Rev. **C64**, 062802 (2001).
- [30] J. Piekarewicz, Phys. Rev. **C62**, 051304 (2000).
- [31] J. Piekarewicz, Phys. Rev. **C69**, 041301 (2004).
- [32] P. Demorest, T. Pennucci, S. Ransom, M. Roberts, and J. Hessels, Nature **467**, 1081 (2010).
- [33] R. J. Furnstahl, Nucl. Phys. **A706**, 85 (2002).
- [34] C. J. Horowitz, S. J. Pollock, P. A. Souder, and R. Michaels, Phys. Rev. **C63**, 025501 (2001).
- [35] K. Kumar, R. Michaels, P. A. Souder, and G. M. Urciuoli (2005), URL <http://hallaweb.jlab.org/parity/prex>.
- [36] J. Piekarewicz, Phys. Rev. **C76**, 031301 (2007).
- [37] J. Piekarewicz, J. Phys. **G37**, 064038 (2010).
- [38] J. Piekarewicz and M. Centelles, Phys. Rev. **C79**, 054311 (2009).
- [39] M. Centelles, X. Roca-Maza, X. Vinas, and M. Warda, Phys. Rev. Lett. **102**, 122502 (2009).
- [40] X. Roca-Maza, M. Centelles, X. Vinas, and M. Warda, Phys. Rev. Lett. **106**, 252501 (2011).
- [41] A. W. Steiner, M. Prakash, J. M. Lattimer, and P. J. Ellis, Phys. Rept. **411**, 325 (2005).